# Symmetry Adapted Approach towards Efficient Trotter Decomposition

Bo Yang[1] and Naoki Negishi[2]
[1] *Graduate School of Information Science and Technology, The University of Tokyo, Bunkyo-ku, Tokyo 113-8656, Japan*
[2] *Graduate School of Arts and Sciences, The University of Tokyo, Meguro-ku, Tokyo, 153-8902, Japan*
(Dated: April 16, 2022)

We simulate the time evolution of the $N = 3$ Heisenberg model on `ibmq_jakarta` with a modified Tritterization scheme based on the circuit level approach (without pulse). Focusing on the symmetry of the $N$-qubit Heisenberg Hamiltonian, we construct an $(N-1)$-qubit effective Hamiltonian. We show the Trotterization of effective Hamiltonian is equivalent to changing the axis of the Trotterization of the original Hamiltonian. When $N = 3$, this encoding framework makes it possible to drastically reduce the number of CNOT gates and the circuit depth into a constant through circuit optimization, regardless of the number of Trotter iterations. Combining with several error mitigation techniques, we finally achieve fidelity $0.9928 \pm 0.0013$ on `ibmq_jakarta` real quantum device, for the given problem setting.

## I. INTRODUCTION

The noisy two-qubit operation and the short coherent time are the two main factors that limits the ability of current near-term quantum computers. Previous researches imply even the depth 10 CNOT gate would destroy the genuine multipartite entanglement on IBM Quantum devices [1, 2]. This problem obviously arises in the given problem setting where we want to simulate the time evolution of Heisenberg model with multiple Trotter iterations.

In fact, the rigorous simulation of the Heisenberg model with Trotterization would result in a deep quantum circuit. According to the sample program [3], one should use over 10 trotter iterations to achieve fidelity over 0.9 under noise-free simulation. In addition, one Trotter iteration in this straightforward method requires at least depth $3 \times 2 = 6$ CNOT gates. When using the `fake_jakarta` noisy simulator, the fidelity could decreased into 0.1 with 12 Trotter iterations. Therefore, making the circuit shallower with less CNOT gates is the top priority to increase the fidelity under the current noise environment.

Towards this, our idea is to focus on the unused symmetry in the given Hamiltonian, which allows us to embed the $N$ sites Heisenberg model into $N-1$-qubit system. Thanks to the commutativity of $XXX$ Heisenberg Hamiltonian $H_{\mathrm{Heis}}$ with all the local Pauli-Z operators, all the eigenvectors of the Heisenberg Hamiltonian have the even degeneracy when the system size $N$ is odd. This induces the relationship between two degenerated orthogonal $m$-th eigenstates $|\phi_-^{(m)}\rangle$ and $|\phi_+^{(m)}\rangle$ as follows. Using this property, we succeed to embed the given $N$ spin Heisenberg Hamiltonian into the equivalent effective Hamiltonian on $N-1$ spin sites by an encoding unitary operator. The Trotterization on the effective Hamiltonian can be seen as taking a different axis of the Trotter decomposition. When the system size is 3, the Trotter circuits only act on the two-qubit system with the same control-target qubits. Therefore, a number of Trotter iterations can be fortunately optimized into constant depth circuit with constant number of CNOT gates, which greatly contributes to simulating the target state with surprisingly high fidelity.

Note that our proposed transformation scheme is "efficently" reduced from the theoretical inspection without any exponential computational cost to the system size $N$. In addition, the proposed method is "end-to-end" Trotterization algorithm which takes $N$-qubit initial state, simulates its time evolution with the modified Trotter axis in one circuit, and outputs the $N$-qubit target state. In this sense, we believe our method satisfies the requirements in the official rules: "Each submission must use Trotterization to evolve the specified state, under the specified Hamiltonian, for the specified duration with at least 4 Trotter steps." [4].

To obtain noiseless results, one may also apply the error mitigation techniques. Error mitigation techniques aims to recover the ideal expectation values via classical post-processing [5]. Here we use quantum readout error mitigation (QREM) and zero-noise exrapolation (ZNE).

The readout noise occurring in the measurement process is one of the significant noise on the current near-term devices. Since this noise can be characterized by an assignment stochastic matrix, we can perform its inverse on the noisy probability distribution. This is the base idea of the QREM method and we use the complete assignment matrix inversion prepared in the Qiskit-Ignis library [6].

We also applied ZNE [7] to the mitigated expectation values by QREM. The ZNE first tests the expectation values with different artificially scaled noise levels, and then extrapolate such noisy expectation values to estimate the "zero-noise" expectation. We used the unitary folding method [8] prepared in the Mitiq library [9]. In addition, we also combined Pauli twirling [10] method with ZNE as applied in [11], where the improvement of the zero-noise expectation values is reported. Here we mitigated all the expectation values use for reconstruct the outcome density matrix. Since

the quantum noise and mitigation noise may output the unphysical density matrix with negative eigenvalues, we found the closest positive semi-definite matrix by the maximum likelihood method [12].

As a result, we achieved the target state **fidelity over 0.99 on the noisy simulator** of `fake_jakarta`, and **over 0.99 on the real quantum device** of `ibmq_jakarta`. We also checked the proposed method can simulate the time evolution from any 3-qubit initial states by both theoretical analysis and experiments. Therefore, we can say that the proposed method not only outputs high scores of the given problem setting of the contest, but also provides a practical solution for the simulation of Heisenberg model using Trotterization under more general situation.

The theoretical insight of the effective Hamiltonian of the Heisenberg model is mainly done by Naoki Negishi. The incorporation of the error mitigation and the code implementation is mainly done by Bo Yang. We solved the problem only by the circuit level optimization, WITHOUT using Qiskit pulse. All the jobs are casted to and retrieved from `ibmq_jakarta` before April 16, 2022. The source code are put at [13] with this report. Since some of the programs use Mitiq library, please install the Mitiq package through 'pip install mitiq' before running them.

## II. THEORETICAL FOUNDATION

Here we will derive the effective Hamiltonian from the given Heisenberg Hamiltonian, focusing on the symmetry of the system. We focused on the 3-site Heisenberg model in this chapter, although general formulation applied for $N$-site Heisenberg model and its time propagation are summarized in Appendix A. We start from the fact that $XXX$ Heisenberg 3-spins Hamiltonian $H_{\mathrm{Heis}}$ is commutable with the products of $\sigma_\mu^i$, $(\mu \in \{x, y, z\})$ for all sites as

$$[H_{\mathrm{Heis}}, \sigma_\mu^1 \sigma_\mu^2 \sigma_\mu^3] = 0. \tag{1}$$

This Hamiltonian can be decomposed as a direct sum of the subspace

$$H_{\mathrm{Heis}} \in \mathcal{H}_{\mathrm{odd}} \oplus \mathcal{H}_{\mathrm{even}}, \tag{2}$$

and $\mathcal{H}_{\mathrm{odd}}$, $\mathcal{H}_{\mathrm{even}}$ is the subspace composed by the eigenstates of $\sigma_z^1 \sigma_z^2 \sigma_z^3$ equal to $-1, 1$, that is

$$\mathcal{H}_{\mathrm{odd}} = \{|100\rangle, |010\rangle, |001\rangle, |111\rangle\} \tag{3}$$
$$\mathcal{H}_{\mathrm{even}} = \{|110\rangle, |101\rangle, |011\rangle, |000\rangle\}. \tag{4}$$

Here any eigenvectors $|\mathrm{odd}\rangle \in \mathcal{H}_{\mathrm{odd}}$ of $H_{\mathrm{Heis}}$ and the vector $\sigma_x^1 \sigma_x^2 \sigma_x^3 |\mathrm{odd}\rangle \in \mathcal{H}_{\mathrm{even}}$ is degenerated. To identify these two states with each other, we introduce the encoding operator $U_{\mathrm{enc}}$ given by

$$\begin{aligned} U_{\mathrm{enc}} = \sigma_x^1 \sigma_x^2 \frac{1 - \sigma_z^3 + \sigma_x^3 - i\sigma_y^3}{2} \times P_{23} \times \frac{1 - \sigma_z^1 \sigma_z^2 \sigma_z^3}{2} \\ + \frac{1 + \sigma_z^3 + \sigma_x^3 + i\sigma_y^3}{2} \times P_{23} \times \frac{1 + \sigma_z^1 \sigma_z^2 \sigma_z^3}{2}. \end{aligned} \tag{5}$$

And projecting this operator to the 3-qubit states, we obtain

$$U_{\mathrm{enc}} |000\rangle = |000\rangle \tag{6}$$
$$U_{\mathrm{enc}} |011\rangle = |001\rangle \tag{7}$$
$$U_{\mathrm{enc}} |110\rangle = |010\rangle \tag{8}$$
$$U_{\mathrm{enc}} |101\rangle = |011\rangle \tag{9}$$
$$U_{\mathrm{enc}} |111\rangle = |100\rangle \tag{10}$$
$$U_{\mathrm{enc}} |100\rangle = |101\rangle \tag{11}$$
$$U_{\mathrm{enc}} |001\rangle = |110\rangle \tag{12}$$
$$U_{\mathrm{enc}} |010\rangle = |111\rangle \tag{13}$$

where $P_{ij}$ is exchange operator between $i$ site and $j$ site and $U_{\mathrm{enc}}^\dagger$ corresponds to decoding operator. The first and second term projecting the state in the subspace $\mathcal{H}_{\mathrm{odd}}$ and $\mathcal{H}_{\mathrm{even}}$ respectively. Focusing on the property, we introduce effective Hamiltonian $H_{\mathrm{eff}}$ which gives the time evolution of the state $|\psi\rangle_{\mathrm{eff}} := U_{\mathrm{enc}} |\psi\rangle$. The time-dependent Schrödinger equation (TDSE) is governed by $H_{\mathrm{eff}}$ as follows

$$i\partial_t |\psi(t)\rangle_{\mathrm{eff}} = H_{\mathrm{eff}} |\psi(t)\rangle_{\mathrm{eff}}, \tag{14}$$

and $H_{\text{eff}}$ is constructed as

$$H_{\text{eff}} = \sigma_x^1 + \sigma_x^2 + \sigma_z^1 + \sigma_z^2 - (\sigma_z^1\sigma_x^2 + \sigma_x^1\sigma_z^2), \tag{15}$$

consistently equal to the TDSE under the $H_{\text{Heis}}$ in the 3-spins system. $\psi(t)$ is the wavefunction. Note that this effective Hamiltonian $H_{\text{eff}}$ is equivalent to the given Hamiltonian $H_{\text{Heis}}$ (see Appendix B), so we do not modified the specified Hamiltonian in this contest. Therefore, the time propagation is described by $\exp(-iH_{\text{eff}}t)$. We Trotterize this time evolution operator into

$$\begin{aligned}\exp(-iH_{\text{eff}}t) &= \exp\left[-it\left\{(\sigma_x^1 + \sigma_z^2 - \sigma_x^1\sigma_z^2) + (\sigma_x^2 + \sigma_z^1 - \sigma_x^2\sigma_z^1)\right\}\right] \\ &= \lim_{n\to\infty}\left[e^{\frac{-it}{n}(\sigma_x^1+\sigma_z^2)}e^{\frac{it}{n}(\sigma_x^1\sigma_z^2+\sigma_x^2\sigma_z^1)}e^{\frac{-it}{n}(\sigma_x^2+\sigma_z^1)}\right]^n.\end{aligned} \tag{16}$$

Both of the first and third Trotter block can be given by local rotation-Z and rotation-X gates for each qubit. The second Trotter block is represented as $4\times 4$ matrix given by

$$\exp\left[\frac{it}{n}(\sigma_x^1\sigma_z^2 + \sigma_z^1\sigma_x^2)\right] = \begin{pmatrix} \cos^2\frac{t}{n} & i\sin\frac{t}{n}\cos\frac{t}{n} & i\sin\frac{t}{n}\cos\frac{t}{n} & \sin^2\frac{t}{n} \\ i\sin\frac{t}{n}\cos\frac{t}{n} & \cos^2\frac{t}{n} & -\sin^2\frac{t}{n} & -i\sin\frac{t}{n}\cos\frac{t}{n} \\ i\sin\frac{t}{n}\cos\frac{t}{n} & -\sin^2\frac{t}{n} & \cos^2\frac{t}{n} & -i\sin\frac{t}{n}\cos\frac{t}{n} \\ \sin^2\frac{t}{n} & -i\sin\frac{t}{n}\cos\frac{t}{n} & -i\sin\frac{t}{n}\cos\frac{t}{n} & \cos^2\frac{t}{n} \end{pmatrix} \tag{17}$$

This matrix is given by a 2-qubit circuit as the figure below (FIG.1).

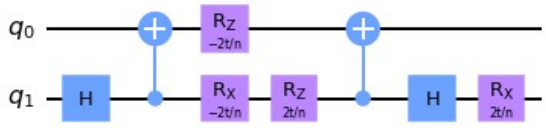


FIG. 1. The quantum gate of the second Trotter block given by Eq.(26)

Including with the first and third trotter blocks in Eq.(16) into the second, the unit of the Trotter step is represented as FIG.2.

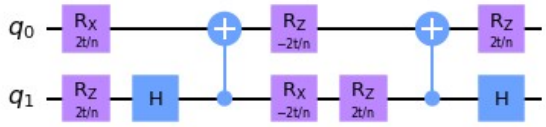


FIG. 2. The quantum gate of the Trotter unit given by Eq.(25)

The last task is the encoding and decoding of the initial and final state, respectively. In our method, we identify the 8 states in 3-spin states with the product between no time-evolving one particle state $|a\rangle_{\text{stat}}$ and time-evolving two-particle state $|bc\rangle_{\text{eff}}$under $H_{\text{eff}}^{23}$ given by Eq.(B8), as follows. where $U_{\text{enc}}$ is the unitary operator to promote encoding, and the decoder of that is given by $U_{\text{enc}}^{\dagger}$. By the encoding and decoding, the circuit for the general solution of the time evolution under $H_{\text{Heis}}$ can be represented as FIG.3

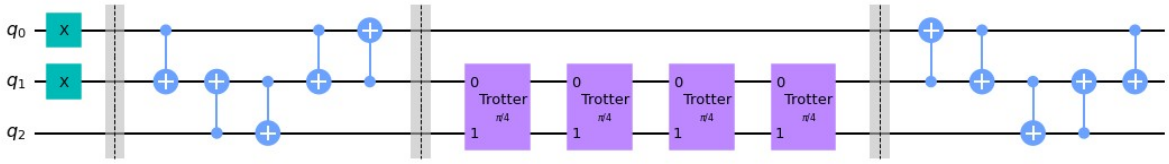


FIG. 3. The circuit gives the general solution of the time evolution by using Trotterization in this approach. Note that the number of Trotter steps on this figure is $n = 4$ case.

## III. STRATEGIES: REDUCING CNOT GATE IN ENCODING AND DECODING

We made the general method of the time evolution governed by $H_{\text{Heis}}$, calling as "**General** encoding(decoding)". Ideally, the circuit in FIG.3 guarantees the exact time evolution in any initial state under $n \to \infty$. However, because the quantum gate of the encoding and decoding need to set 5 CNOT gates for each when we use ibm-jakarta, the noises are not perfectly removed for the high state tomography fidelity. In this section, we show the strategies to get much higher fidelity by reducing CNOT gates in encoding and decoding process by adapting the initial state conditions and time duration.

### A. Considering initial condition:"Shallow encoding and Specific decoding"

In this contest, the initial state is chosen as not entangled state, $|011\rangle$. This means that the encoding process **never** required CNOT gate in this method, and we call this encoding strategy as "**Shallow** encoding". Moreover, the time evolution is closed in the subspace $\mathcal{H}_{\text{even}}$ as choosing $|011\rangle$ in initial state. It is only need to consider the decoding process as 4 states given by

$$
\begin{aligned}
|000\rangle &= U_{\text{enc}}^{\dagger} |000\rangle \\
|011\rangle &= U_{\text{enc}}^{\dagger} |001\rangle \\
|110\rangle &= U_{\text{enc}}^{\dagger} |010\rangle \\
|101\rangle &= U_{\text{enc}}^{\dagger} |011\rangle .
\end{aligned}
$$

We focused on this boundary condition to reduce the CNOT gate for the decoding, calling as "**Specific** decoding". The circuit in this strategy is given by FIG.4, where the only two CNOT gates are needed.

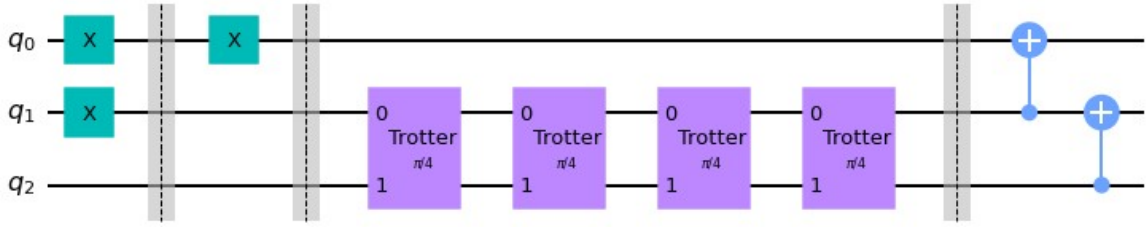


FIG. 4. The circuit giving the specific solution of the time evolution by using Trotterization of the $H_{\text{Heis}}$ in this approach considering initial condition and subspace. Note that the number of Trotter steps on this figure is $n = 4$ case.

### B. Considering periodic time evolution

Although the state vector $\psi(t)$ generally cannot match the initial state $\psi(0)$ generated by more three eigenvectors, the state completely returns to the initial state in a certain period if any gaps between $i$ and $j$-th eigenenergies $\Delta_{ij}$ are equal to the integer multiplication of a certain real value. Focusing on this property, we can further reduce CNOT gates in the decoding process, so called "**Shallow** decoding". In the case of $H_{\text{Heis}}$, we can easily prove that $\Delta_{ij}$ is

equal to even number without diagonalizing the $8 \times 8$ matrix. By introducing a vector of total Pauli matrix defined as

$$\boldsymbol{\sigma}^{\mathrm{tot}} = \boldsymbol{\sigma}^1 + \boldsymbol{\sigma}^2 + \boldsymbol{\sigma}^3, \tag{18}$$

where $\boldsymbol{\sigma}^{\mathrm{i}} := (\sigma_x^i, \sigma_y^i, \sigma_z^i)$. The Hamiltonian is reconstructed as

$$\begin{aligned} H_{\mathrm{Heis}} &= \frac{1}{2}(\boldsymbol{\sigma}^{\mathrm{tot}})^2 - \boldsymbol{\sigma}^1 \cdot \boldsymbol{\sigma}^3 - \frac{1}{2}\sum_i (\boldsymbol{\sigma}^i)^2 \\ &= \frac{1}{2}(\boldsymbol{\sigma}^{\mathrm{tot}})^2 - \boldsymbol{\sigma}^1 \cdot \boldsymbol{\sigma}^3 - \frac{9}{2} \\ &= \frac{1}{2}(\boldsymbol{\sigma}^{\mathrm{tot}})^2 - \frac{1}{2}(\boldsymbol{\sigma}^1 + \boldsymbol{\sigma}^3)^2 - \frac{3}{2} \end{aligned} \tag{19}$$

And we can show the commutation relation as

$$[H_{\mathrm{Heis}}, \boldsymbol{\sigma}^{\mathrm{tot}}] = 0. \tag{20}$$

It indicates that the task is only to find the eigenenergies of $(\boldsymbol{\sigma}^1 + \boldsymbol{\sigma}^3)^2$ if we know that of $(\boldsymbol{\sigma}^{\mathrm{tot}})^2$. The eigenvalue of $(\boldsymbol{\sigma}^{\mathrm{tot}})^2$ is well known and given by

$$\langle (\sigma^{\mathrm{tot}})^2 \rangle = S^{\mathrm{tot}}(S^{\mathrm{tot}} + 2), \tag{21}$$

where $S^{\mathrm{tot}}$ =3 or =1. The eigenvalue of $(\boldsymbol{\sigma}^1 + \boldsymbol{\sigma}^3)^2$ is also given by Eq.(21) with $S^{\mathrm{tot}} = 2$ or $= 0$. Then, substituting $(\boldsymbol{\sigma}^{\mathrm{tot}})^2$ =15 or =3, and $(\boldsymbol{\sigma}^1 + \boldsymbol{\sigma}^3)^2$ =8 or =0, respectively, we can say $\Delta_{ij} \in 2\mathbb{Z}$ which guarantees that the state in this system perfectly returns to initial state, and the period is equal to the integer multiplication of $\pi$. It means that regarding the decoding process can be regarded as inverse operation of encoding process in $t \in \pi\mathbb{Z}$ case. If we set the initial state as $|011\rangle$, the circuit can be represented by FIG.4. In such case, we can encode and decode without CNOT gate.

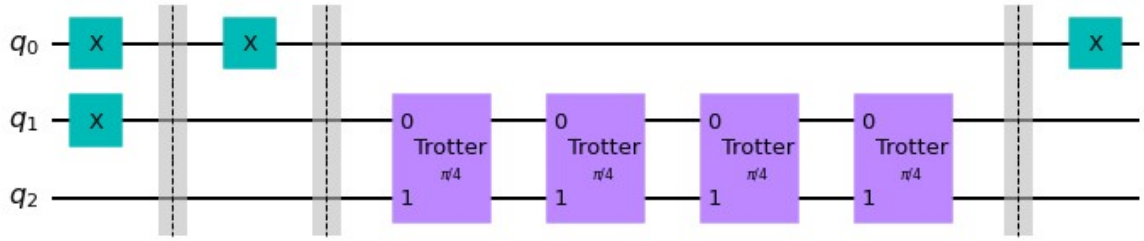


FIG. 5. The circuit giving the specific solution of the time evolution by using Trotterization of the $H_{\mathrm{Heis}}$ in this approach considering initial condition, subspace and time dulation $t \in \pi\mathbb{Z}$. Note that the number of Trotter steps on this figure is $n = 4$ case.

## IV. EXPERIMENTS

In this section, we will see the proposed method works correctly and outputs high fidelity through some experimental results. The experiments are performed on three different backends of `qasm_simulator`, `fake_jakarta`, and `ibmq_jakarta`. The `qasm_simulator` provides the noise-free simulation, `fake_jakarta` provides the noisy simulation that mimics the actual noises on `ibmq_jakarta`, and `ibmq_jakarta` is the real quantum backend of IBM Quantum Jakarta. All the circuits ran with 8192 shots, and the fidelity are averaged over 8 repeated tries.

### A. Results from Noise-free Simulator

First, to justify the correctness of the proposed method, we performed the numerical simulations on noise-free simulator `qasm_simulator`. We chose the initial state as the equal superposition of $|010\rangle$ and $|110\rangle$, and evolved it

from $t = 0$ to $t = [0, \pi/20, 2\pi/20, \cdots, \pi]$. Clearly, since the state $|010\rangle + |110\rangle$ is in the space of $\mathcal{H}_{\text{odd}} \oplus \mathcal{H}_{\text{even}}$, we used the quantum circuit in FIG. 3. At each target time, the probability of state $|010\rangle + |110\rangle$ is computed as the sample code [3] did.

The result is shown in FIG. 6. In this figure, the red curve denotes the theoretical probability computed by the rigorous Trotter decomposition of given Heisenberg Hamiltonian. The green plots denote the simulated values at each time step by the proposed method using the effective Hamiltonian. We can see all the simulation results are almost on the theoretical curves, which not only confirms the correctness of our method but also supports the generality on the initial state in 3-qubit system.

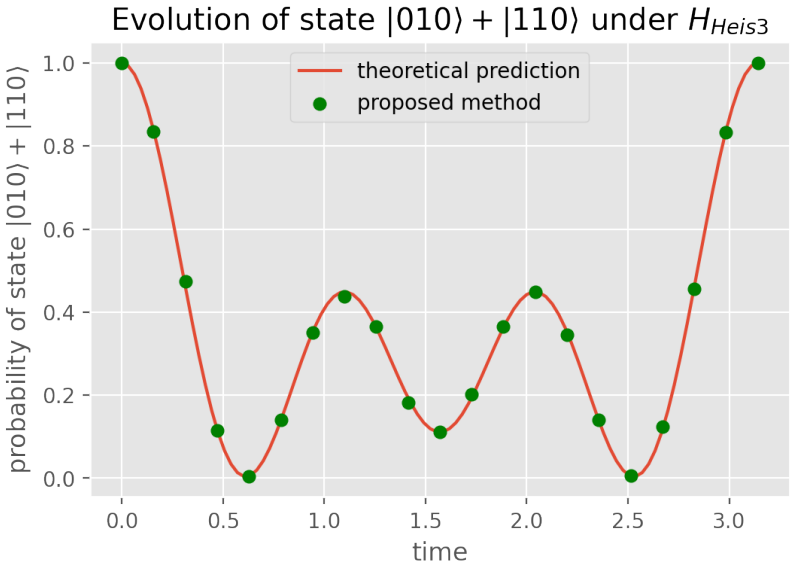


FIG. 6. This figure compares the theoretical time evolution and the evolution simulated by the proposed method, over the 3-qubit Heisenberg model.

### B. Results from Noisy Simulator

Next, we performed the noisy simulation on `fake_jakarta`. Here we ere to compute the fidelity of the target state after the evolution time $\pi$ from the given initial state $|110\rangle$. To reduce the noise effect, we added several quantum error mitigation (QEM) techniques.

One method is the quantum readout error mitigation (QREM) applied to the noisy probability distribution. Here we adopt the complete measurement calibration and mitigation, using 'complete_meas_cal' and 'CompleteMeasFitter' in Qiskit-Ignis. In addition, the zero-noise extrapolation (ZNE) is also added to the process. We use the linear fitting method 'LinearFactory' in Mitiq with the scale factors 1.0, 2.0 and 3.0. This will triple the number of circuits to be implemented. As a result, the whole workflow with QREM and ZNE is shown in FIG.7. Furthermore, the Pauli twirling technique is also combined with ZNE. This is to add random local Pauli gates around the CNOT gates in the circuits. We refer to the implementation of Pauli twirling by [11].

While the 'StateTomographyFitter' class is used for recovering the density matrix from the tomography circuits in the sample program [3], this class only takes probability distributions of tomography circuits. Since the outputs of ZNE are expectation values, we made a new function that takes expectation values of tomography circuits and outputs the recovered density matrix. As a side note, the sample program uses the least square method in the 'StateTomographyFitter' to find the closest physically valid density matrix. In our self-made function, we used the method by [12].

On `fake_jakarta`, we examined the performance of the different encoding and decoding strategies with different Trotter steps. Here we applied QREM to noisy results before computing the fidelity. FIG. 8 (a) shows the results by both general encoding and decoding, shallow encoding and specific encoding, and both shallow encoding and decoding. We tried the Trotter steps with $[1, 2, 3, 4, 5, 6, 7, 8, 9, 10, 20, 30, 40]$ in this experiment. The gap and the recovery of the fidelity around 4-step case exhibit the same trend as the naive Trotter decomposition in the sample code [3]. This also imply the proposed method runs within the scope of Trotterization approaches.

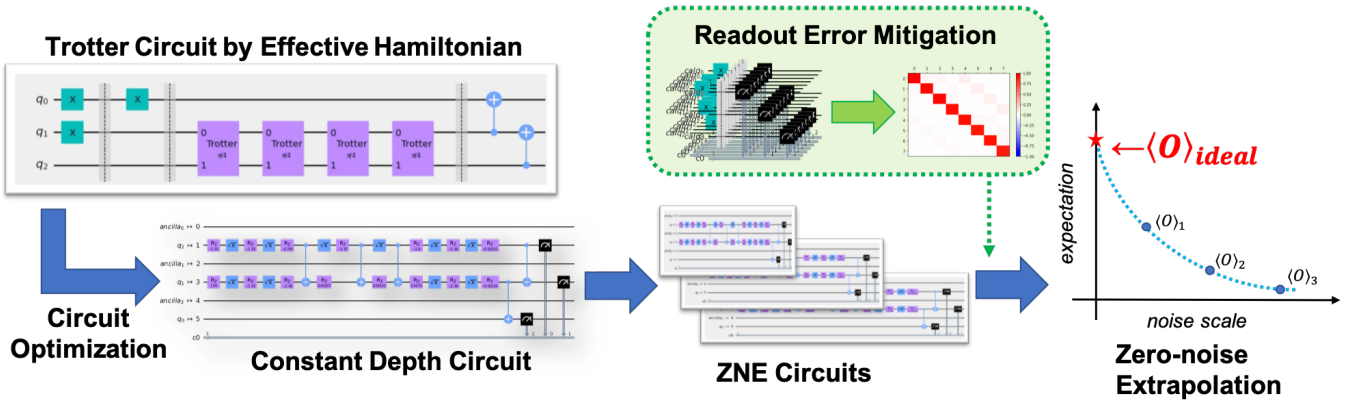


FIG. 7. The workflow of the whole process to obtain the expectation value on each Pauli measurement for the state tomography. When we use ZNE, the density matrix is recovered from each expectation value of Pauli measurement. When we do not use ZNE, the probability distributions after QREM will be directly passed to the 'StateTomographyFitter'.

The effect of QEM methods is also investigated. This time, we fix the setting into shallow encoding and specific decoding. We can know from FIG. 8 (b) that all the QEM methods may contribute to the increase of the fidelity. From both figures, it is also clear that 30 Trotter iterations are enough for high approximation rate by Trotterization.

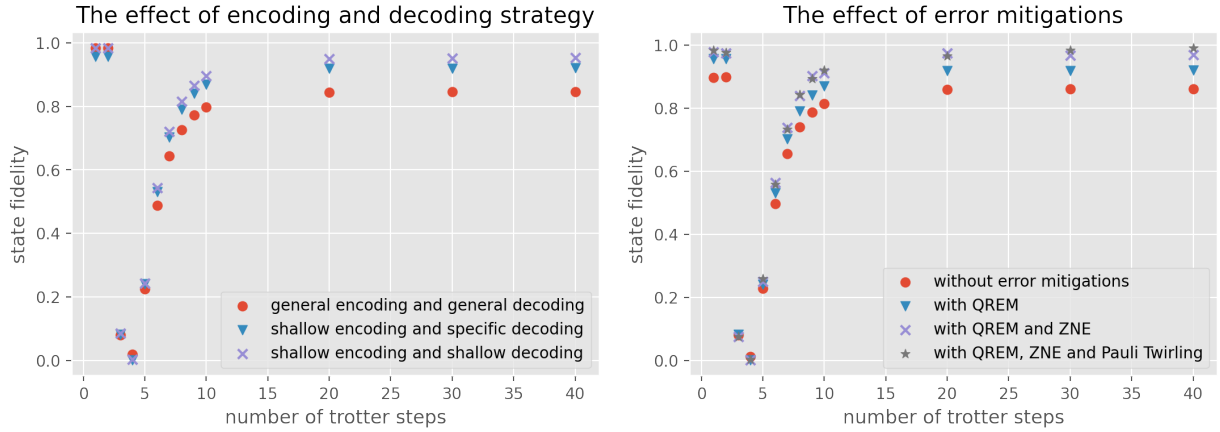


FIG. 8. (a) The left figure shows the comparison of different encoding strategy with different number of Trotter iterations. (b) The right figure compares the effect of adding different levels of error mitigation techniques, also with different number of Trotter iterations.

### C. Results from IBM Quantum Jakarta

Finally, we will see the results from the real quantum device, `ibmq_jakarta`. We run the circuits with 100 trotter steps, with and without the error mitigation under different encoding and decoding methods. The result are listed up on TABLE I. In this table, fidelities from `fake_jakarta` and `ibmq_jakarta` are compared. All the fidelities exceed 0.80 on `ibmq_jakarta`. With QREM, all the fidelities even exceed 0.90. In particular, it is notable that the raw fidelity by shallow encoding and decoding scores over 0.99 on `ibmq_jakarta`, only applying QREM.

## V. CONCLUSION

In conclusion, we achieved the fidelity over 0.99 on IBM Quantum Jakarta device for the given problem settings and within the rules. This is greatly thanks to the symmetry of the given Heisenberg Hamiltonian, which allows us to perform Trotterization on the effective Hamiltonian.

| Settings | `fake_jakarta` | `ibmq_jakarta` |
|---|---|---|
| **General encoding and general decoding** | | |
| without any QEM | $0.7856 \pm 0.0015$ | $0.8039 \pm 0.0048$ |
| with QREM | $0.8448 \pm 0.0015$ | $0.9032 \pm 0.0054$ |
| with QREM and ZNE | $0.9393 \pm 0.0053$ | $0.9866 \pm 0.0017$ |
| with QREM, ZNE and Pauli Twirling | $0.9801 \pm 0.0031$ | - |
| **Shallow encoding and specific decoding** | | |
| without any QEM | $0.8631 \pm 0.0017$ | $0.8637 \pm 0.0041$ |
| with QREM | $0.9234 \pm 0.0016$ | $0.9728 \pm 0.0040$ |
| with QREM and ZNE | $0.9840 \pm 0.0024$ | $0.9857 \pm 0.0043$ |
| with QREM, ZNE and Pauli Twirling | $0.9714 \pm 0.0048$ | $0.9624 \pm 0.0167$ |
| **Shallow encoding and shallow decoding** | | |
| without any QEM | $0.8863 \pm 0.0012$ | $0.8803 \pm 0.0044$ |
| with QREM | $0.9533 \pm 0.0017$ | $0.9852 \pm 0.0061$ |
| with QREM and ZNE | $0.9855 \pm 0.0036$ | $0.9929 \pm 0.0015$ |
| with QREM, ZNE and Pauli Twirling | $0.9801 \pm 0.0031$ | $0.9768 \pm 0.0034$ |

TABLE I. Fidelities of the target state from IBM Quantum Jakarta and its fake simulator under different settings. Fortunately, we witnessed even higher score $0.9928 \pm 0.0013$ for shallow encoding and decoding with QREM, and using 15 Trotter steps.

For the further improvements, we can increase the shot count of readout calibration circuits to mitigate the readout error more precisely. The general framework for $N$-qubit case is also left for the future work. We suspect our method might be possible to be extended to efficient simulation of $N$-qubit Heisenberg models, while some restrictions on the generality might be imposed.

## ACKNOWLEDGMENTS

We would like to thank all the organizing staffs of this contest for holding this event and for their hard work. In particular, we are very grateful to AJ Rasmusson for his kind replies and clear answers on our questions about the clarification of the official rules.

[1] B. Yang, R. Raymond, and S. Uno, An efficient quantum readout error mitigation for sparse measurement outcomes of near-term quantum devices (2022).
[2] G. J. Mooney, G. A. L. White, C. D. Hill, and L. C. L. Hollenberg, Journal of Physics Communications **5**, 095004 (2021).
[3] IBM Quantum Awards: Open Science Prize 2021, `https://github.com/qiskit-community/open-science-prize-2021` (2021).
[4] Official Rules of IBM Quantum Awards: Open Science Prize 2021, `https://res.cloudinary.com/ideation/image/upload/w_870/jug8tjgy6egm26zojyxd.pdf` (2021).
[5] S. Endo, Z. Cai, S. C. Benjamin, and X. Yuan, Journal of the Physical Society of Japan **90**, 032001 (2021).
[6] G. Aleksandrowicz, T. Alexander, P. Barkoutsos, L. Bello, Y. Ben-Haim, D. Bucher, F. J. Cabrera-Hernández, J. Carballo-Franquis, A. Chen, C.-F. Chen, J. M. Chow, A. D. Córcoles-Gonzales, A. J. Cross, A. Cross, J. Cruz-Benito, C. Culver, S. D. L. P. González, E. D. L. Torre, D. Ding, E. Dumitrescu, I. Duran, P. Eendebak, M. Everitt, I. F. Sertage, A. Frisch, A. Fuhrer, J. Gambetta, B. G. Gago, J. Gomez-Mosquera, D. Greenberg, I. Hamamura, V. Havlicek, J. Hellmers, Łukasz Herok, H. Horii, S. Hu, T. Imamichi, T. Itoko, A. Javadi-Abhari, N. Kanazawa, A. Karazeev, K. Krsulich, P. Liu, Y. Luh, Y. Maeng, M. Marques, F. J. Martín-Fernández, D. T. McClure, D. McKay, S. Meesala, A. Mezzacapo, N. Moll, D. M. Rodríguez, G. Nannicini, P. Nation, P. Ollitrault, L. J. O'Riordan, H. Paik, J. Pérez, A. Phan, M. Pistoia, V. Prutyanov, M. Reuter, J. Rice, A. R. Davila, R. H. P. Rudy, M. Ryu, N. Sathaye, C. Schnabel, E. Schoute, K. Setia, Y. Shi, A. Silva, Y. Siraichi, S. Sivarajah, J. A. Smolin, M. Soeken, H. Takahashi, I. Tavernelli, C. Taylor, P. Taylour, K. Trabing, M. Treinish, W. Turner, D. Vogt-Lee, C. Vuillot, J. A. Wildstrom, J. Wilson, E. Winston, C. Wood, S. Wood, S. Wörner, I. Y. Akhalwaya, and C. Zoufal, Qiskit: An Open-source Framework for Quantum Computing (2019).
[7] K. Temme, S. Bravyi, and J. M. Gambetta, Phys. Rev. Lett. **119**, 180509 (2017).
[8] T. Giurgica-Tiron, Y. Hindy, R. LaRose, A. Mari, and W. J. Zeng, in *2020 IEEE International Conference on Quantum Computing and Engineering (QCE)* (IEEE, 2020).
[9] R. LaRose, A. Mari, N. Shammah, P. Karalekas, and W. Zeng, Mitiq: A software package for error mitigation on near-term quantum computers, `https://github.com/unitaryfund/mitiq` (2020).
[10] Y. Li and S. C. Benjamin, Phys. Rev. X **7**, 021050 (2017).

[11] N. F. Berthusen, T. V. Trevisan, T. Iadecola, and P. P. Orth, Quantum dynamics simulations beyond the coherence time on nisq hardware by variational trotter compression (2021).
[12] J. A. Smolin, J. M. Gambetta, and G. Smith, Phys. Rev. Lett. **108**, 070502 (2012).
[13] N. N. Bo Yang, Solutions for ibm quantum open science prize 2021, `https://github.com/BOBO1997/osp_solutions` (2022).

## Appendix A: Extending the effective Hamiltonian for $N$-sites Hisenberg model

## Appendix B: Projection operator in encoding and the evolution operator given by the effective Hamiltonian.

Making two projection operators $P_+$, $P_-$ introduced by respecting the operator $U_{\mathrm{enc}}$ in Eq.(5) as

$$P_+ = \frac{1+\sigma_z^3+\sigma_x^3+i\sigma_y^3}{2} \times P_{23} \times \frac{1+\sigma_z^1\sigma_z^2\sigma_z^3}{2} \tag{B1}$$

$$P_- = \sigma_x^1\sigma_x^2 \frac{1-\sigma_z^3+\sigma_x^3-i\sigma_y^3}{2} \times P_{23} \times \frac{1-\sigma_z^1\sigma_z^2\sigma_z^3}{2}, \tag{B2}$$

we can rewrite $H_{\mathrm{Heis}}$ as

$$H_{\mathrm{Heis}} = \sum_{i\in\{+,-\}} P_i^\dagger H_{\mathrm{eff}} P_i. \tag{B3}$$

The projection operator satisfies the following relations,

$$P_+ \in \mathcal{H}_{\mathrm{even}}, P_- \in \mathcal{H}_{\mathrm{odd}} \tag{B4}$$

$$P_+P_-^\dagger = P_-P_+^\dagger = P_+^\dagger P_- = P_-^\dagger P_+ = 0 \tag{B5}$$

$$P_+^\dagger P_+ = I_+ \in \mathcal{H}_{\mathrm{even}} \tag{B6}$$

$$P_-^\dagger P_- = I_- \in \mathcal{H}_{\mathrm{odd}} \tag{B7}$$

$$H_{\mathrm{eff}} \in \mathcal{H}_{\mathrm{odd}} \oplus \mathcal{H}_{\mathrm{even}}, \tag{B8}$$

where $I_{+,-}$ is identity operator in the subspace $\mathcal{H}_{\mathrm{even,odd}}$, respectively. where $I_+$ and $I_-$ is identity operator in the subspace $\mathcal{H}_{\mathrm{even}}$ and $\mathcal{H}_{\mathrm{odd}}$, respectively. Because $P_+^\dagger H_{\mathrm{eff}} P_+$ and $P_-^\dagger H_{\mathrm{eff}} P_-$ are commutable, the time evolution operator $\exp(-iH_{\mathrm{Heis}}t)$ can be exactly separated into two parts,

$$\begin{aligned}\exp(-iH_{\mathrm{Heis}}t) &= \sum_{i\in\{+,-\}} P_i^\dagger \exp(-iH_{\mathrm{eff}}t)P_i \\ &= (P_+ + P_-)^\dagger \exp(-iH_{\mathrm{eff}}t)(P_+ + P_-).\end{aligned} \tag{B9}$$

Then we derived the time propagation is given by the effective Hamiltonian.

## Appendix C: Device information of IBM Quantum Brooklyn

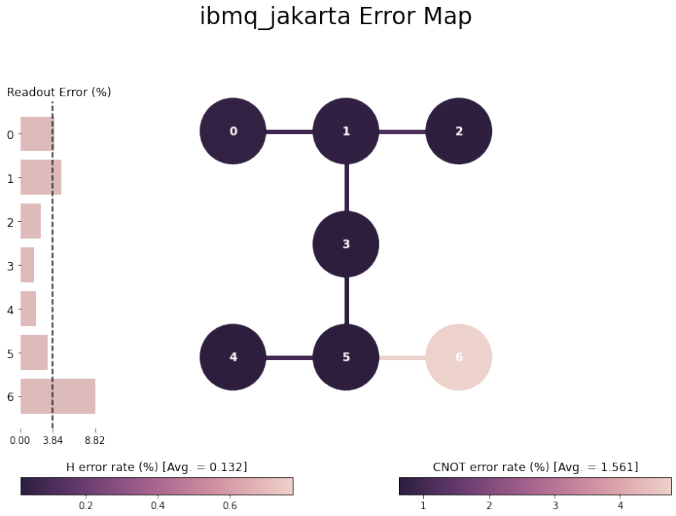


FIG. 9. This figure is reflects the error map of ibmq_jakarta at 11 p.m. (UTC+9) on April 16, 2022. The numbers on the figure represent the positions of physical qubits. We use the physical qubit 5, 3, and 1 as virtuial qubit position 0, 1, and 2.